Inorganic Chemistry

Article

pubs.acs.org/IC

Synthesis of Porphyrin–CdSe Quantum Dot Assemblies: Controlling Ligand Binding by Substituent Effects

Isabelle Chambrier, Chiranjib Banerjee, Sonia Remiro-Buenamañana, Yimin Chao, Andrew N. Cammidge,* and Manfred Bochmann*

School of Chemistry, University of East Anglia, Norwich Research Park, Norwich NR4 7TJ, U.K.

Supporting Information

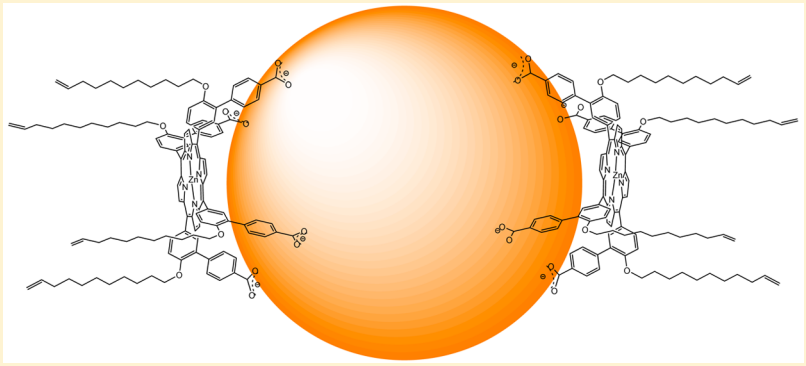

ABSTRACT: Cadmium selenide quantum dots of 2.2–2.3 nm diameter were prepared by phosphorus-free methods using oleic acid as stabilizing surface ligand. Ligand exchange monitored quantitatively by ^{1}H NMR spectroscopy gave an estimate of 30–38 monodentate ligands per nanocrystal, with a ligand density of 1.8–2.3 nm^{-2}. The extent of ligand exchange with macrocycles carrying one or more functional groups was investigated, with the aim of producing nanocrystal–macrocycle conjugates with a limited number of coligands. Metal-free porphyrins are able to sequester the Cd^{2+} ions from the $Cd(oleate)_2$ outer layer of the nanocrystals. Zinc porphyrin complexes carrying one carboxylate function displace oleate efficiently to give porphyrin/CdSe composites with porphyrins stacked upright on the crystal surface. Porphyrins with four potential ligating sites are able to bind to the crystal surface only if the donors are at the end of sufficiently long and flexible tethers. High-dilution methods allowed the synthesis and isolation of well-defined composites of composition [CdSe{porphyrin}$_2$], where porphyrin = 5,10,15,20-tetrakis{3-(carboxy-*n*-alkyloxy)phenyl}porphyrinato zinc (n = 5 or 10) and 5,10,15,20-tetrakis{3-(11-undecenyloxythiol)phenyl}-porphyrinato zinc. Comparison of the composition data obtained by ^{1}H NMR spectroscopy with luminescence quenching behavior suggests a dependence of quenching efficiency on the tether length. Luminescence quenching was also observed for porphyrins that, according to ^{1}H NMR results, do not undergo surface ligand exchange.

INTRODUCTION

The arrangement of nanosized objects into more complex structures remains a challenging target.[1−3] One of the preconditions for such higher level organization is the introduction of a limited number of attachment points. This offers the opportunity to link up spherical nanoparticles using covalent bonds or specific donor–acceptor interactions to generate, for example, divalent[4] or trivalent nanoparticles that can be the building blocks for linear or branched arrangements. For gold nanoparticles monofunctionalization and binary linkers have been realized in a number of cases.[5]

We were especially interested in the functionalization of colloidal semiconductor quantum dots (QDs), in particular CdSe, and were looking for ways of restricting the number of surface ligands by macrocyclic attachments, using coordination chemistry principles for the construction of stable nanocrystal–organic conjugates. The successful functionalization of nanoparticles requires an understanding of their surface chemistry. Semiconductor nanocrystals are stabilized by surfactant-type surface ligands which determine the growth rate, stability, and solubility of the nanocrystals.[6] For example, while CdSe prepared using trioctylphosphine (TOP) and trioctylphosphine oxide (TOPO) are frequently represented with a surface coverage of TOPO, it is now known that the surface is mainly covered by TOP oxidation products, alkyl phosphinates and phosphonates,[7−10] which coordinate to metal surface sites as bridging ligands.[11] As such they can be difficult to displace in ligand exchange reactions.[11−13]

Nanocrystals prepared under phosphorus-free conditions using long-chain carboxylic acids such as stearic or oleic acid are stabilized by a layer of metal carboxylate.[14] The nature of ligand binding has been explored mainly by NMR spectroscopy,[15,16] as well as luminescence[17] and isotopic labeling[18] methods.

Received: April 22, 2015
Published: July 14, 2015

DOI: 10.1021/acs.inorgchem.5b00892
Inorg. Chem. 2015, 54, 7368–7380

Chart 1

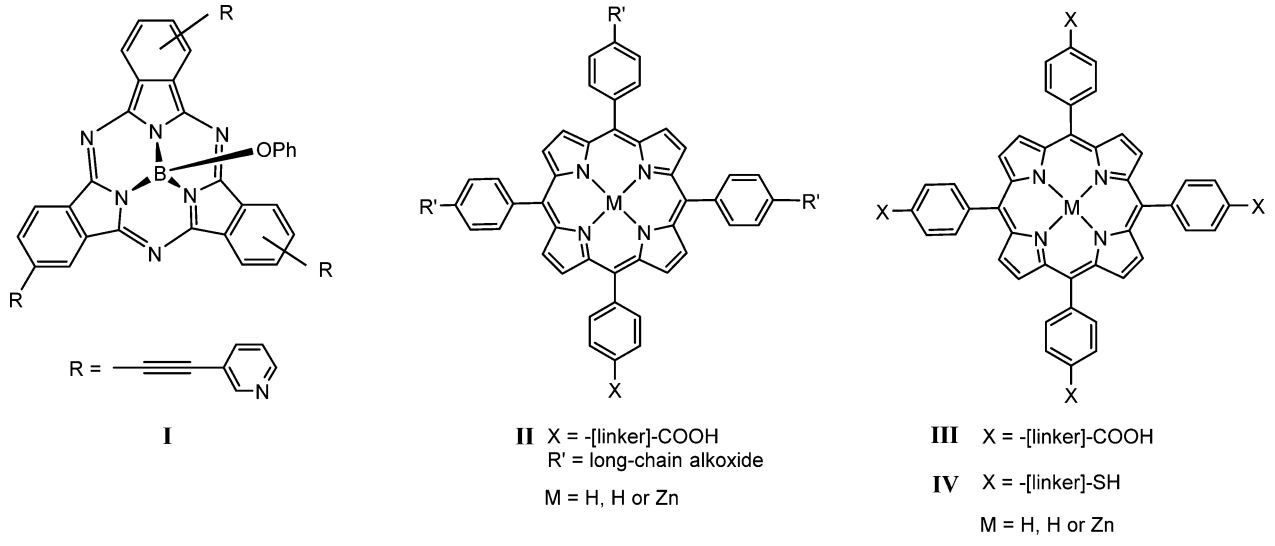

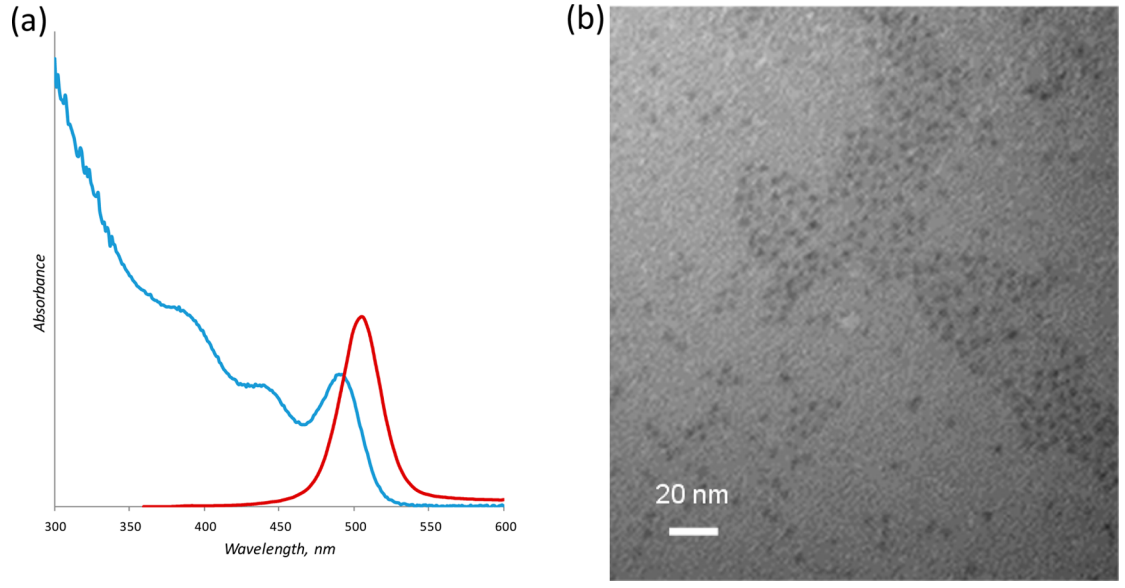

Figure 1. (a) Typical UV−vis (blue) and fluorescence (red) spectra of CdSe nanoparticles used in this study ($CHCl_3$ solution). (b) Transmission electron microscopy (TEM) image of this CdSe sample.

These carboxylate ligand spheres show dynamic behavior in solution and undergo a multitude of ligand exchange reactions,[15,19,20] although the preparation of heteroligated nanocrystals at the synthesis stage has also been reported.[21]

Macrocyclic compounds with a rigid aromatic framework, such as phthalocyanines, subphthalocyanines, and porphyrins, are synthetically readily accessible and can easily be derivatized to give compounds with a predetermined number of anchor points (usually 0−4). Such ligands are expected to bind to nanocrystal surface sites by substitution of the surfactant ligands present from the synthesis stage. For a given concentration, due to the chelate effect polydentate ligands should bind to the surface of a nanocrystal significantly more strongly than monodentate ligands. In continuation of our synthetic and structural investigations of porphyrin and phthalocyanine systems,[22] we decided to focus on ligands of types **I**−**IV** for the present study (Chart 1). Subphthalocyanines **I** possess a cup-shaped structure,[23] which suggested a good geometric match with nanocrystals with diameters in the 2−3 nm range; in addition they contain a functional group perpendicular to the macrocyclic core which offers the possibility of connecting to other ligand-decorated nanoparticles by covalent bonds. Porphyrins of type **II** would be expected to act as monodentate ligands oriented perpendicular to the nanocrystal surface. On the other hand, although the central ring in porphyrins of type **III** is flattened, there is sufficient flexibility both in the ring and in the functionalized substituents X to allow these compounds to attach themselves to nanocrystals flat-on, i.e., parallel to the crystal surface. Alternatively these ligands may adopt a perpendicular orientation bridging between two adjacent quantum dots. The structures and properties of the CdSe−macrocyclic constructs have been evaluated using a combination of ^{1}H NMR, absorption, and fluorescence spectroscopies.

DOI: 10.1021/acs.inorgchem.5b00892
Inorg. Chem. 2015, 54, 7368−7380

RESULTS AND DISCUSSION

CdSe Nanoparticle Preparation. Although CdSe quantum dots are frequently synthesized using trioctylphosphine (TOP)/trioctylphosphine oxide (TOPO) as coordinating solvent and surfactants, as discussed in the Introduction,[6−10] the surface chemistry of these nanoparticles is not well-defined. We therefore favored a modified octadecene (ODE)/oleic acid (OA) method,[24,25] especially because there were fewer uncertainties concerning the composition of the ligand surface. The CdSe nanocrystals used in this study were prepared using CdO, oleic acid in octadecene (ODE), and Se powder, following the method of Jasieniak et al.[24] This method produced highly monodisperse particles, coated exclusively with oleate ligands. The particles are readily soluble in chloroform, and all ligand exchange reactions described here were carried out in that solvent. Typical examples of UV−vis and fluorescence spectra are shown in Figure 1a. The diameter of the nanoparticles (d = ca. 2.2−2.3 nm, confirmed by TEM, Figure 1b)[26] and the solution concentration were calculated from the UV absorption maximum using the method by Yu et al.[27] A fluorescence quantum yield (QY) of ca. 3% was measured by a comparative method described by Williams et al.[28] using quinine sulfate in 0.1 N H_2SO_4 as reference (QY = 54.6%).

Relative Ligand Binding Strength. Oleic acid (octadec-9-enoic acid) possesses a *cis*-vinylene moiety which acts as a convenient ^{1}H NMR marker. Because of the inhomogeneity of surface binding sites and enhanced relaxation times, the vinylene signal of surface-bound oleate is broad,[15,21] without a detectable coupling pattern, but sharpens when oleate is released. Preliminary qualitative experiments served to establish the relative binding preference of carboxylic acids, phosphonic acids, and thiols in our system and showed the sequence

$$RCOO^- < RPO_3H_2 \approx RSH < R{-}PO_3^{2-} < RS^-$$

For example, both dodecanethiol and 11-undecenylphosphonic acid quantitatively displace oleate from the CdSe surface. However, it was not possible to displace surface-bound alkylphosphonate by thiol, unless triethylamine was added as a base to generate equilibrium concentrations of the more nucleophilic thiolate anion.

On the other hand, competition experiments using equimolar mixtures of dodecanethiol and 11-undecenylphosphonic acid gave nanoparticles which showed a S:P ratio of 3:1 in the absence of NEt_3. Under such conditions the exchange presumably involves the hydrophosphonate anion, $R'PO_3H^-$ (eq 1). On addition of NEt_3, however, the S:P ratio of the CdSe ligand sphere increased to 11:1, demonstrating preferential binding of thiolate under basic conditions.[29]

$$CdSe(O_2CR)_x + yR'PO_3H_2 + zR''SH \underset{x=y+z}{\rightleftharpoons} CdSe(SR'')_z(R'PO_3H)_y + xRCOOH \quad (1)$$

In these reactions 11-undecenylphosphonic acid was chosen since the terminal $-CH{=}CH_2$ unit provides another ^{1}H NMR marker; its ^{1}H NMR signal occurs conveniently in a clear part of the spectrum. Upon the first additions to an excess of CdSe in solution, the terminal double bond signals shifted slightly upfield. Although remote from the anchoring point, the double bond signal shows the typical broadening effect induced by binding to the nanocrystal surface.

These experiments also demonstrated that phosphonate binding cannot be assessed by ^{31}P NMR spectroscopy since no ^{31}P NMR signal was observed for phosphonate-exchanged CdSe; liberation of the phosphonate by a dodecanethiol/NEt_3 mixture was required in order to detect the ^{31}P NMR signal. For this reason the surface coverage of our ligand-exchanged quantum dots was always assessed by purification followed by quantitative displacement with thiolate.

Number of Ligands per Nanoparticle. The number of oleate ligands per nanoparticle and hence the ligand density was evaluated using a combination of UV−vis and ^{1}H NMR spectroscopies. The ^{1}H NMR spectrum of the pure nanoparticles shows a broad signal at ca. δ 5.3 assigned to the *cis*-CH═CH protons of the bound oleate ligands. When attached to a solid particle, the resulting slow motion and the diverse chemical environments the molecules experience lead to broadening of the peaks. The effect is especially pronounced for the atoms closest to the surface whose signals can sometimes be shifted or disappear.[21,30] Several methods were employed for monitoring and measuring surface coverage and exchange. For the as-prepared nanoparticles, introduction of a known quantity of an NMR integration standard (ferrocene, sharp singlet at δ 4.16, $CDCl_3$) allows direct calculation of surface coverage by integration of the broad δ 5.3 ppm signal. For 2.0 nm particles the average surface coverage is calculated as 30 oleate ligands per particle (see Supporting Information). For other ligands, the native oleates were exchanged by titration; the release of oleic acid from the surface is accompanied by the appearance of a sharp signal of free oleic acid in solution and addition was continued until no further sharpening of the free oleic acid signal was observed. A typical example is shown for 11-bromoundecanoic acid in Figure 2, and the results, presented in Table 1, show the range of calculated results over a number of nanoparticle synthesis and exchange sequences. The values of ligand density obtained in Table 1 could, in principle, be affected by the ligand exchange dynamics, especially in the case of acid−acid exchange. However, thiols, which quantitatively displace carboxylates

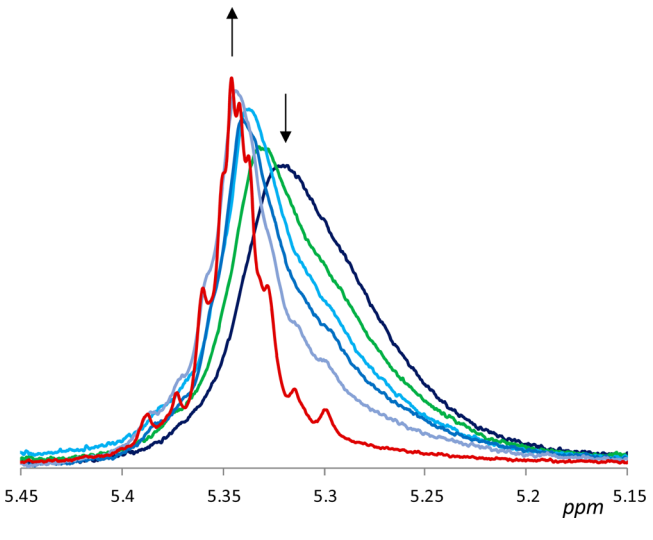

Figure 2. ^{1}H NMR resonances of the vinylene protons of the oleate ligands upon successive additions of 11-bromoundecanoic acid (0−50 equiv). The arrows indicate the decrease of the broad signal of surface-bound oleate at δ 5.3 and its replacement with the signal for free oleic acid at δ 5.35 as the result of surface ligand substitution.

DOI: 10.1021/acs.inorgchem.5b00892
Inorg. Chem. 2015, 54, 7368−7380

Table 1. Estimated Values of Ligand Densities from Ligand Exchange as Observed by ^{1}H NMR Spectroscopy

	ligands per QD	ligand density (nm^{-2})
11-bromoundecanoic acid	33−38	1.95−2.25
dodecanethiol	32−47	1.9−2.8
4,5-didodecylphthalic acid	14−18	0.8−1.1
oleic acid[a]	30	1.8

[a]As-prepared nanoparticles (2.0 nm diameter) measured against ferrocene as NMR integration standard.

from Cd chalcogenide nanoparticles,[6] yielded a similar calculated ligand density and thus confirmed the values found by carboxylate exchange. As a multidentate ligand, 4,5-didodecylphthalic acid is expected to bind more strongly than monodentate ligands[31] and displace two oleates, which is what was found. All measurements show good agreement. The values calculated are lower than that obtained by Hens and co-workers (4.6 nm^{-2})[15c] but are in agreement with those found by Anderson and Owen (2.0−2.9 nm^{-2})[32] for carboxylate-ligated CdSe nanocrystals of similar size.

Assuming a ratio of Cd:Se per nanoparticle of ca. 1.15:1,[7,33] a molecular formula of $Cd_{128}Se_{111}$ can be derived for nanoparticles of d = 2.3 nm. Comparing the number of oleate ligands to the excess cadmium per CdSe quantum dot (17), a ratio of ca. 2:1 was obtained, i.e., the surface excess of Cd^{2+} is balanced by a double amount of oleate ligands as reported earlier by Hens,[15c] giving an average composition of our CdSe particles as $[Cd_{111}Se_{111}\{CdX_2\}_{17}]$ (X = oleate).

The area per molecule of a Langmuir film of oleic acid was measured by Tomoaia-Cotisel et al. as A_0 = 41 Å^2 on water (pH = 2).[34] By comparison, stearic acid yielded a lower area per molecule of A_0 = 20 Å^2 under the same conditions. The kink induced by the *cis*-double bond in oleic acid is believed to be the cause of this increase in area. The authors confirmed these results through calculations taking into account the van der Waals radius of H and obtained an area comprised between 36.0 and 41.0 Å^2. Based on these "footprint" data, we can calculate the maximum number of oleate ions that could comfortably be accommodated on the surface of a nanoparticle of d = 2.3 nm as 39−45, i.e., a density of 2.4−2.8 nm^{-2}. Our data in Table 1 fall below this value and are therefore consistent. The collapse pressure, i.e., the pressure at which the monolayer becomes unstable, was established at an area per molecule of 27 Å^2. Using this value, a maximum density of 3.7 nm^{-2} would be obtained for a very condensed system.

Reactions of Subphthalocyanines with CdSe QDs. In a series of initial reactions, the binding behavior of subphthalocyanine **I** (Chart 1) was explored. This ligand is decorated with three *meta*-pyridyl substituents which give a bite angle that should be geometrically well-matched for binding to nanocrystals of 2−3 nm diameter, provided there are accessible Lewis acidic surface sites. Treatment of a solution of CdSe QDs in chloroform gave a deeply colored solution. Quenching of the QDs fluorescence was observed. The nanoparticles were precipitated with methanol, isolated by centrifugation, and repeatedly washed with acetone until the washings were free of subphthalocyanine by UV/vis spectroscopy. Subsequent analysis by ^{1}H NMR spectroscopy showed, however, that the peaks of the residual SubPc contained in the sample were neither broadened nor shifted, indicating that the SubPc was not bound but probably trapped in the forest of aliphatic chains of oleic acid. Unsubstituted SubPc also induced quenching of QDs fluorescence (vide infra).

Carboxylate-coated nanoparticles of the type used here have two pathways for ligand substitution, the displacement of an X^- (oleate) anion, or displacement of surface-bound CdX_2. The latter pathway would have to be operative in the case of neutral donors like pyridine-decorated sub-Pc. Evidently, at least with carboxylate-terminated nanoparticles, this pathway is not competitive.

Reaction of Metal-Free Porphyrin Derivatives with CdSe Nanoparticles. The interaction of pyridine-substituted free-base porphyrins as well as their metal complexes with CdSe and Cd/ZnS core−shell particles made by the TOPO route has been intensively studied, especially by Zenkevich and

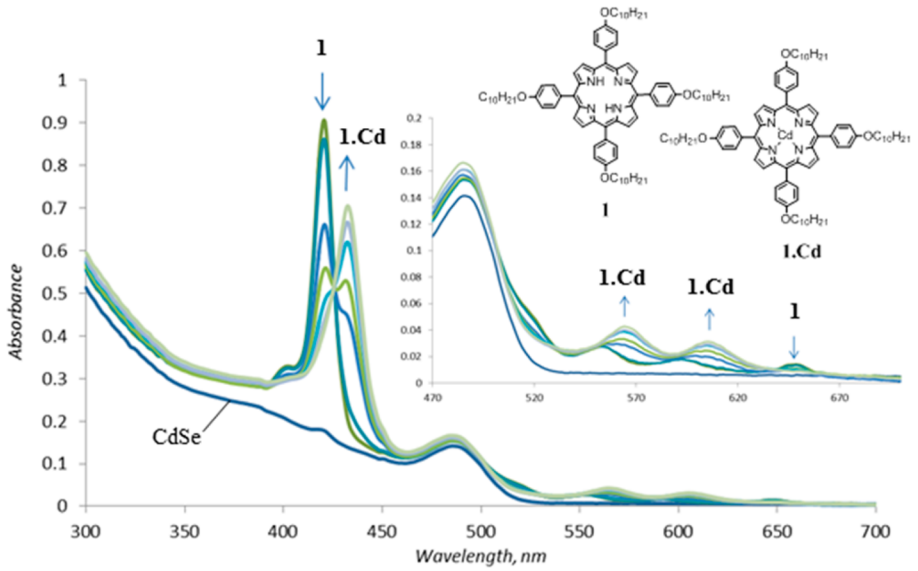

Figure 3. Conversion of metal-free 5,10,15,20-tetra(4-decyloxyphenyl)porphyrin (**1**) to 5,10,15,20-tetra(4-decyloxyphenyl)porphyrinato cadmium in the presence of CdSe nanoparticles over time (room temperature, CH_2Cl_2) (dark blue line, CdSe alone, λ_{max} 486 nm; metal-free porphyrin, λ_{max} 420 nm; cadmium porphyrin, λ_{max} 433 nm; time = 0, 1, 16, 24, 40, 64, 140 h).

DOI: 10.1021/acs.inorgchem.5b00892
Inorg. Chem. 2015, 54, 7368−7380

others.[35−37] We were therefore interested in the interactions of carboxylate-type CdSe nanocrystals with carboxylate-substituted porphyrins.

Preliminary studies were carried out with 5,10,15,20-tetra(4-decyloxyphenyl)porphyrin[38] (**1**) (Figure 3), which carries only alkyl substituents but no surface-binding functional groups. It quickly became evident that metal-free porphyrins become metalated in the presence of CdSe nanoparticles over time at room temperature. The insertion of Cd^{2+} into the ring system was evidenced by a visible color change; this was confirmed by the UV−vis spectra. Figure 3 shows the conversion of the metal-free **1** into 5,10,15,20-tetra(4-decyloxyphenyl)-porphyrinato cadmium as a typical example. In fact all metal-free porphyrins in this work behaved similarly, whether these were designed to bind to the nanoparticles or not. The Soret band shifts from 420 to 433 nm, and this is accompanied by the characteristic Q-band reduction from 4 to 2 absorption peaks that can be seen in the inset. It was further established that only the excess Cd^{2+} on the surface of the nanoparticles reacts in this way, as the reaction stops when these are depleted, even though excess porphyrin-H_2 is present.

The metalation of tetraphenylporphyrins by metal films has been observed before; in these cases the macrocycle was obviously able to bind face-on to the metal surface.[39] This is evidently not possible in this case. Metal sequestration by porphyrins that are not capable of coordinating directly to the nanoparticle surface is possible only if surface-bound CdX_2 is part of a solution equilibrium, which is shifted by Cd^{2+} uptake by the macrocycle (eqs 2 and 3), in line with observations by Anderson et al.[16c]

$$CdSe(CdX_2)_x \rightleftharpoons CdSe(CdX_2)_{x-1} + CdX_2 \quad (2)$$

$$CdX_2 + porphH_2 \rightarrow Cd(porph) + 2HX \quad (3)$$

Consequently, the work described hereafter was carried out using zinc metalated porphyrin molecules.

Monodentate Porphyrin Ligands and CdSe Nanoparticles. The binding of monodentate porphyrin ligands was first examined (Figure 4). The macrocycles were functionalized with a single carboxylic acid function that would act as the anchoring point. 5-(4-Carboxyphenyl)-10,15,20-triphenylporphyrinato zinc (**2**) was synthesized using a modified literature procedure.[16]

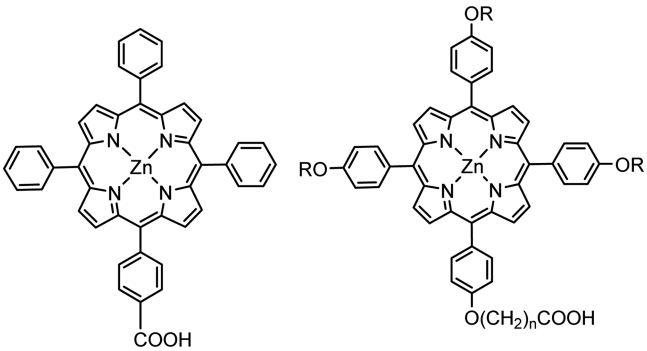

Figure 4. Structures of monodentate porphyrin ligands **2**−**4**.

The ligand exchange process was assessed by ^1H NMR spectroscopy. Aliquots of a solution of **2** were added to a solution of CdSe and NMR spectra obtained after each addition. After ca. 20 equiv of **2** had been added, the signals characteristic of free oleic acid in solution started to appear. The contents of the tube was transferred to a centrifuge tube, methanol was added to flocculate the nanoparticles, and the mixture was centrifuged. Porphyrin **2** is soluble in methanol, and the supernatant was colored. Further washings were required until the UV spectrum of the supernatant confirmed the absence of porphyrin. The nanoparticle sample was dissolved in $CDCl_3$; the resulting ^1H NMR spectrum is shown in Figure 5a. As expected in the case of surface-bound molecules, the signals are very broad; in fact the signals attributed to the phenyl ring bearing the carboxylic function are not visible at all and broadened into the baseline. Adding an excess of dodecanethiol releases the porphyrin and gives the spectrum shown in Figure 5b, along with that of oleic acid. Integration gives a ratio of 1:16 porphyrin:oleate. Based on the average number of surface ligands per nanoparticle determined earlier (Table 1), this equates to about two bound porphyrin molecules per quantum dot.

The addition of 20 equiv of porphyrin was deemed sufficient as we anticipated that not more than half of the oleate ligands would be exchanged due to steric constraints. However, free oleic acid could be fully released in solution as judged from the ^1H NMR spectrum when a very large excess of porphyrin was added (>200 equiv), but the resulting isolated powder could not be redispersed in any solvent.

Quantitative UV experiments showed a small bathochromic shift in absorption of the porphyrin in the presence of CdSe nanoparticles (Figure 6). This was only evident when CdSe was added to an excess of a porphyrin solution.

In order to examine the influence of the length of the tether chain on binding ability and the number of surface-bound porphyrins, two new Zn-porphyrins were synthesized, **3** and **4**, which bear anchoring and solubilizing alkyl chains of different lengths. The synthetic route is shown in Scheme 1.

Aliquots of a solution of porphyrins **3** or **4** (up to ca. 50 equiv) were added to a solution of CdSe, and the binding process was followed by ^1H NMR spectroscopy. Based on the shift and change of shape of the vinyl oleate region signals, it appears that the longer C_{11} chains of **4** are better able to induce release of oleic acid than the shorter C_6 chains of **3**. When additions were complete, the nanoparticle−porphyrin conjugate was isolated and extensively washed with acetone, as described for **2**. The samples were subsequently dried and redissolved in $CDCl_3$. The aromatic region of the ^1H NMR spectrum of **4** (Figure 7a) showed a mixture of broad and sharper peaks. The NMR spectrum of **3** was very similar. Integration of the whole region yielded a value identical to the integration after addition of dodecanethiol, Figure 7b. The inset in Figure 7 shows the signals associated with the $-CH_2-CO_2$ protons of the carboxylic acid function, in surface-bound (lower trace) form and after release with dodecanethiol (upper trace). Integration of the ligand signals after thiol treatment gave a porphyrin:oleate ratio of 4:1 for the shorter chain ligand **3**, and 8:1 for **4**. As can be expected from steric considerations, it is evidently easier for the longer chain ligand to penetrate the oleate ligand shell and undergo ligand exchange. Unlike compound **2**, binding had no effect on the UV absorption spectra of either **3** or **4**.

DOI: 10.1021/acs.inorgchem.5b00892
Inorg. Chem. 2015, 54, 7368−7380

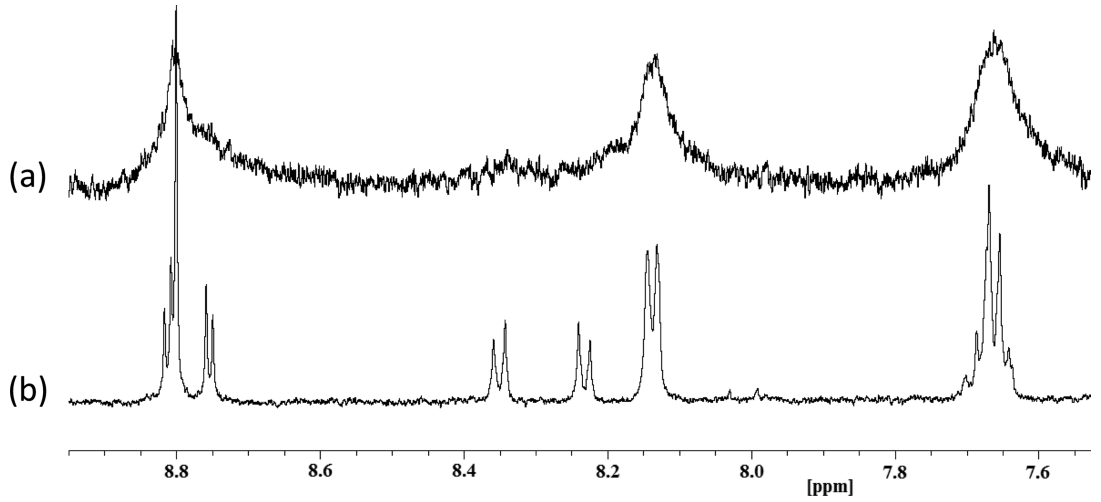

Figure 5. ^{1}H NMR spectra of isolated nanoparticles following the addition of ca. 20 equiv of 5-(4-carboxyphenyl)-10,15,20-triphenylporphyrinato zinc (**2**) in the absence (a) and presence (b) of excess dodecanethiol (7.6−9.1 ppm region).

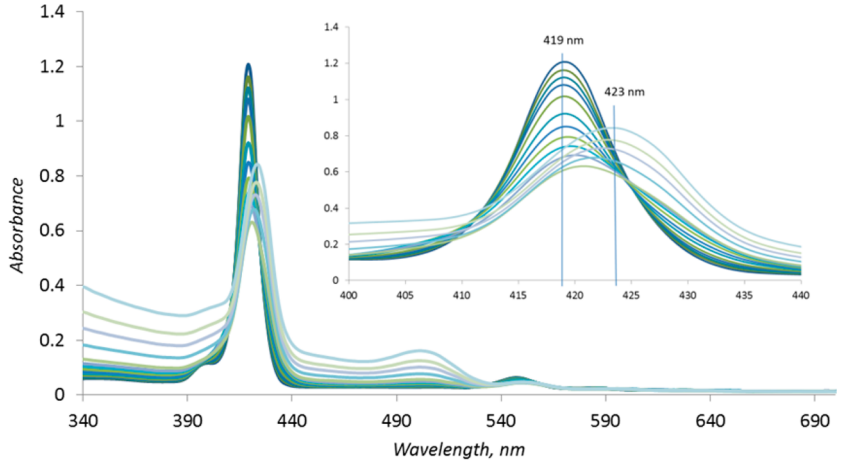

Figure 6. UV/vis spectra of the sequential addition of CdSe to porphyrin **2** showing the bathochromic shift from 419 nm (**2**) to 423 nm (**2** + CdSe).

Tetradentate Porphyrin Ligands and CdSe Nanoparticles. While monodentate porphyrin ligands were readily able to substitute oleate ligands, their steric requirements are moderate since they bind to the nanoparticle surface in "upright" position. Polydentate ligands, on the other hand, have the potential of covering large sections of the nanocrystal surface by lying flat, and we were interested in the question whether or not a nanoparticle could be essentially encapsulated by porphyrins and what binding mode would be adopted. The tetrasubstituted porphyrins **5**−**9** (Figure 8) were therefore synthesized (see Supporting Information for details). In addition to the carboxylate functionalities, porphyrins **5** and **6** carry long chain alkenyloxy substituents to aid solubility, each equipped with a terminal CH═CH_2 moiety that acts as an additional ^{1}H NMR marker. The metalation with Zn had to be achieved as the last step in the synthesis as demetalation occurred during the ester hydrolysis. The use of weakly coordinating organic solvent such as THF or CH_2Cl_2 led to the formation of an insoluble material, probably resulting from the formation of coordination polymers from the interaction of Zn with the carboxylate functions. Consequently, pyridine was used as solvent in the metalation reaction as it appeared to suppress this behavior.

Porphyrins were chosen due to the flexibility of the molecule. It is well-known that, in the case of tetraphenylporphyrins, the phenyl groups in the *meso* positions lie perpendicular to the tetrapyrrolic ring. Such a ligand is therefore able to bind parallel to the nanoparticle surface, as in Figure 9a. Of course, the phenyl substituents are free to rotate, and geometries b, c, and d will also be present.

After addition of ca. 10 equiv of **5** (i.e., 40 equiv of acid functions), there was no evidence by ^{1}H NMR spectroscopy for any binding of this porphyrin **5** to the nanoparticles. The aromatic peaks were slightly shifted downfield relative to the starting material but not broadened, and the oleate signal did not sharpen. This contrasts with the behavior of **2**, which has a similarly short carboxylate linker. This lack of binding could be taken as an indication of the molecule's attempt to lie flat on the nanoparticle surface, without being able to break through and displace the oleate layer. It was clear that a longer tether was required, and compound **6** was prepared.

The reaction of **6** with CdSe caused a precipitate to form which was clearly visible after 1 equiv of **6** was added to the NMR tube. The supernatant was checked by UV/vis spectroscopy and was free of both porphyrin and CdSe. There was clearly an interaction between **6** and the nanoparticles disrupting the stability of the colloidal suspension. The

DOI: 10.1021/acs.inorgchem.5b00892
Inorg. Chem. 2015, 54, 7368−7380

Scheme 1. Preparation of 5-(4-Carboxyhexyl-6-oxyphenyl)-10,15,20-tris(4-decyloxyphenyl)porphyrinato Zinc (3) and 5-(4-Carboxyundecyl-11-oxyphenyl)-10,15,20-tris(4-decyloxyphenyl)porphyrinato Zinc (4)[a]

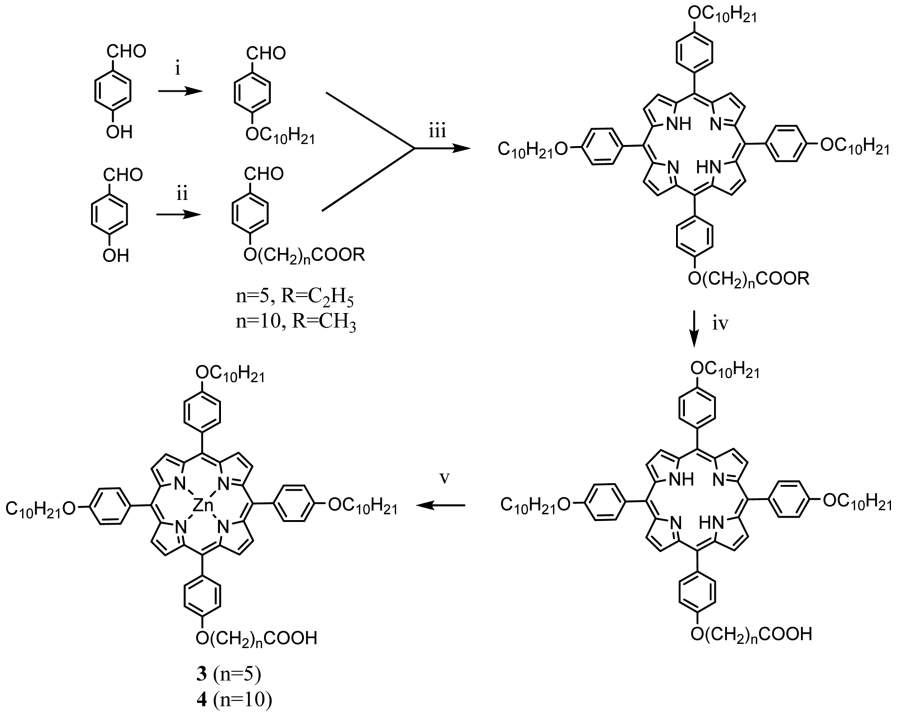

[a]Reagents: (i) K_2CO_3, DMF, $BrC_{10}H_{21}$; (ii) K_2CO_3, DMF, $Br(CH_2)_nCOOR$; (iii) propionic acid, pyrrole; (iv) THF, aqueous NaOH; (v) THF, $Zn(OAc)_2$.

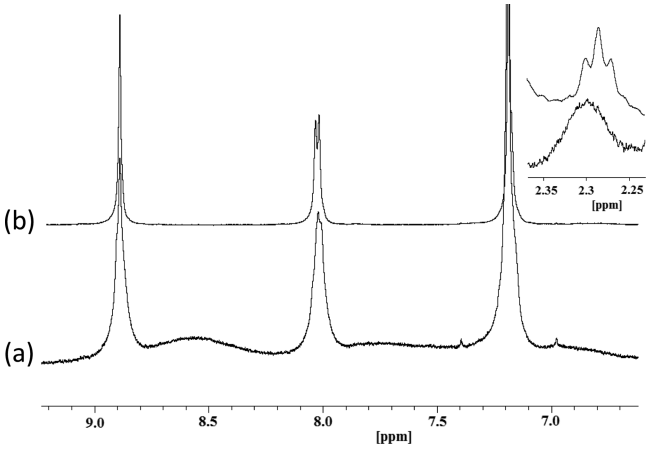

Figure 7. ^{1}H NMR spectra ($CDCl_3$) of isolated and redissolved CdSe nanoparticles coated with **4**: (a) aromatic region; (b) after addition of dodecanethiol. The inset shows the $-CH_2CO_2$ signals before (lower trace) and after addition of dodecanethiol (upper trace).

solid was isolated but could not be redissolved except after addition of dodecanethiol, which released the bound porphyrin from the nanoparticle surface as well as any remaining oleate ligands. A possible binding mode of **6** to the nanoparticle is shown in Figure 10a, which may explain the loss of colloidal stability, despite the presence of the four undecyloxy chains. However, it can also be envisaged that **6** may bridge across two nanoparticles, Figure 10b, which is likely to lead to the formation of a polymeric system, Figure 10c, causing the formation of a precipitate. Indeed it is likely that the polymeric system is prominent in this case. It was in fact possible to bind more porphyrin molecules to the already precipitated material after shaking a suspension of the solid in the presence of more porphyrin, as judged from the absence of porphyrin absorption in the supernatant (UV/vis).

Compounds **7** and **8** (Figure 8) were synthesized to increase the flexibility of the alkyl chains carrying the carboxylic acid functions (for details see Supporting Information).

Aliquots of a solution of porphyrin **8** in THF-d_8 were added to a solution of CdSe in $CDCl_3$ (9 mg in 0.5 mL), and the ^{1}H NMR spectra were recorded after each addition (Figure 11). All the aromatic proton signals are very broad and almost disappear into the baseline, which indicates that all four $-C_6H_4(CH_2)_{10}COOH$ substituents must interact with the nanoparticles equally strongly. A precipitate was observed after the addition of 2 equiv of porphyrin. In this case, due to the presence of THF-d_8, the oleate signals shifted upfield upon successive additions (relative to the peak of residual $CHCl_3$), and sharpened, as expected for exchanging free and coordinated oleates. Porphyrin **7** behaved identically.

Because of the long flexible anchoring chains in these compounds it was not unexpected that the resulting [CdSe-{porphyrin}$_n$] assemblies should show a tendency to cross-link and form insoluble polymeric systems. A high-dilution strategy was therefore applied. 2 equiv of **8** was slowly added to a very dilute CdSe solution (0.04 mg/mL) over a 16 h period. This produced a clear solution free of any solid precipitate. The solvent was then removed, leaving a 5−10 mL volume, which was transferred to a centrifuge tube. The nanoparticle assembly was precipitated with methanol and separated by centrifugation. The resulting solid was washed several times with acetone until the washings were clear (UV/vis), and then dried. The dried material was readily soluble in $CDCl_3$. The NMR spectra of the [CdSe{porphyrin}] assembly (Figure 12) appeared totally featureless in the aromatic region, implying that **8** was attached

DOI: 10.1021/acs.inorgchem.5b00892
Inorg. Chem. 2015, 54, 7368−7380

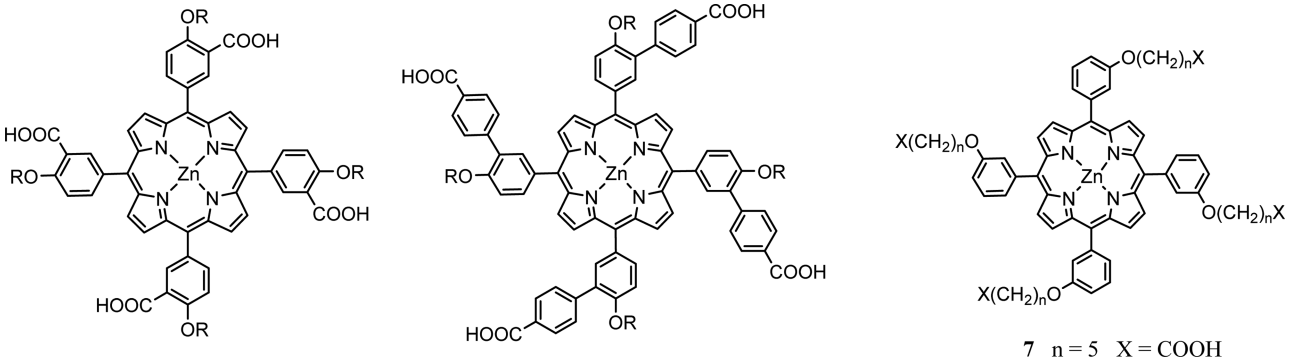

5 R = $(CH_2)_9CH{=}CH_2$ **6** R = $(CH_2)_9CH{=}CH_2$

7 n = 5 X = COOH
8 n =10 X = COOH
9 n =11 X = $SCOCH_3$

Figure 8. Structures of tetradentate porphyrin ligands **5**–**9**.

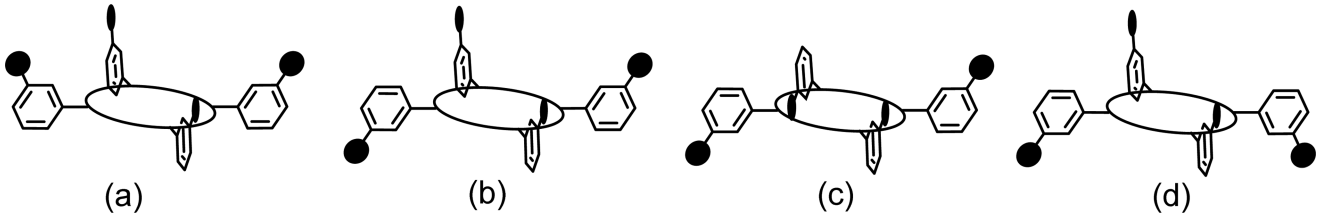

Figure 9. Schematic representation of the possible geometries adopted by a tetrasubstituted porphyrin molecule bearing 4 anchoring points. The clear circle represents the tetrapyrrolic ring, while the dark circles indicate the anchoring points.

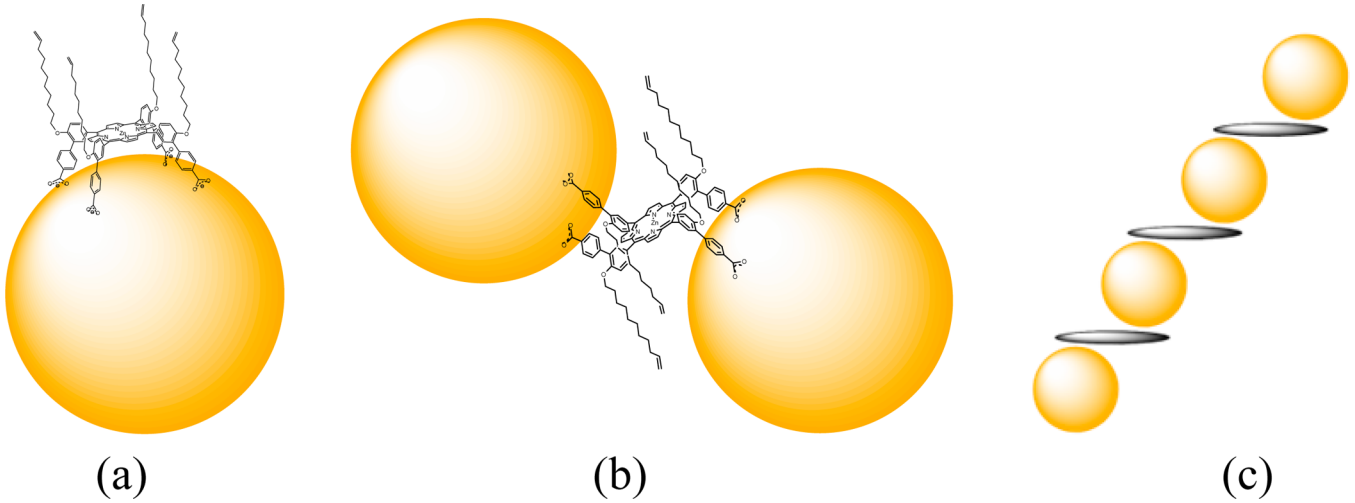

Figure 10. Schematic representation of possible interactions of **6** and CdSe nanoparticles.

to individual nanocrystals in tetradentate fashion. The porphyrin and oleate ligands could be liberated upon addition of dodecanethiol. Peak integration yielded an oleate:porphyrin ratio of ca. 15:1, consistent with the coordination of two tetradentate porphyrins per nanoparticle, and since all aromatic ^{1}H NMR signals are subject to the same amount of broadening, a face-down coordination mode is indicated. The results also highlight the importance of retaining a large proportion of the original oleate ligands to ensure adequate solubility.

The TEM images of these [CdSe{porphyrin}] conjugates showed no indication of aggregation. Together with the NMR evidence this confirms the formation of well-defined porphyrin:CdSe assemblies where the porphyrin is bound by tetradentate ligation.

Since thiol ligands show the highest binding constants for coordinating to CdSe nanocrystal surfaces, the possibility of generating a tetrathiol porphyrin was explored. Since polythiols are very prone to oxidation and form insoluble disulfides, porphyrin **9** (Figure 8) was prepared as the tetra(thioacetate), with the deprotection and formation of the −SH compound left to the last step, just prior to the addition to the nanoparticles. The deprotection has to be carried out under strictly anaerobic conditions (see Supporting Information for details). Similar compounds have been used in the literature for binding onto gold surfaces, but the deprotection step was always carried out in situ.[40] About 2 equiv of the deprotected porphyrin was added slowly overnight to a dilute solution of CdSe (0.04 mg/mL) in the presence of BHT (= 4-Me-2,6-$Bu^t_2C_6H_2OH$) as antioxidant. A clear solution was obtained

DOI: 10.1021/acs.inorgchem.5b00892
Inorg. Chem. 2015, 54, 7368−7380

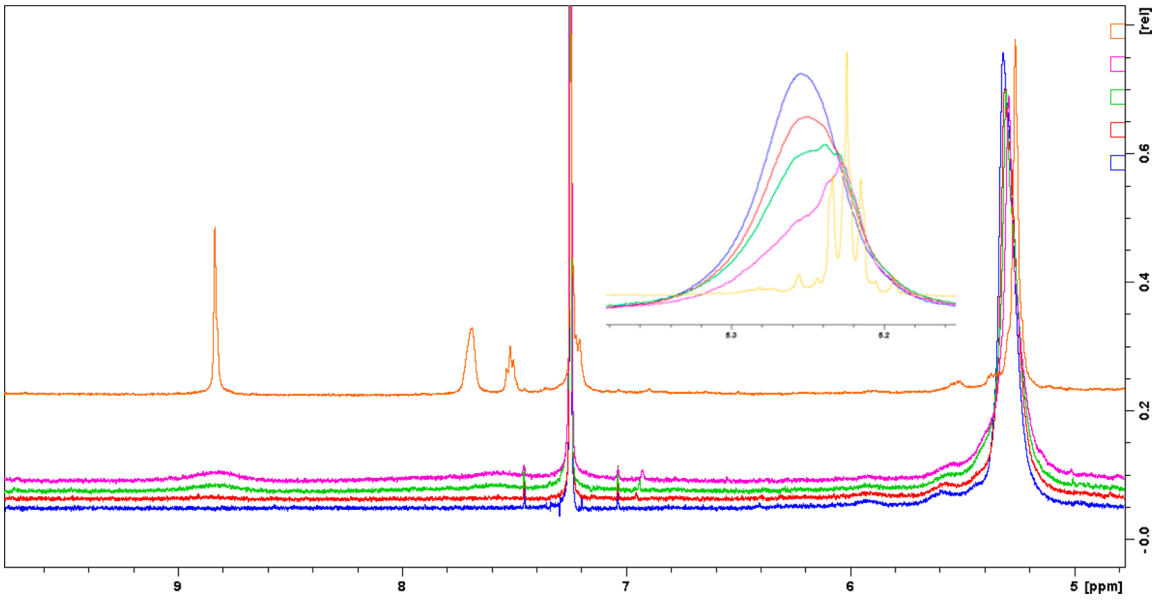

Figure 11. ^{1}H NMR spectra (5−10 ppm region) recording the addition of **8** in THF-d_8 to CdSe nanoparticles in $CDCl_3$. Blue: CdSe alone. Red: 0.5 equiv added. Green: 1 equiv added. Pink: 2 equiv added. Orange: after adding excess dodecanethiol.

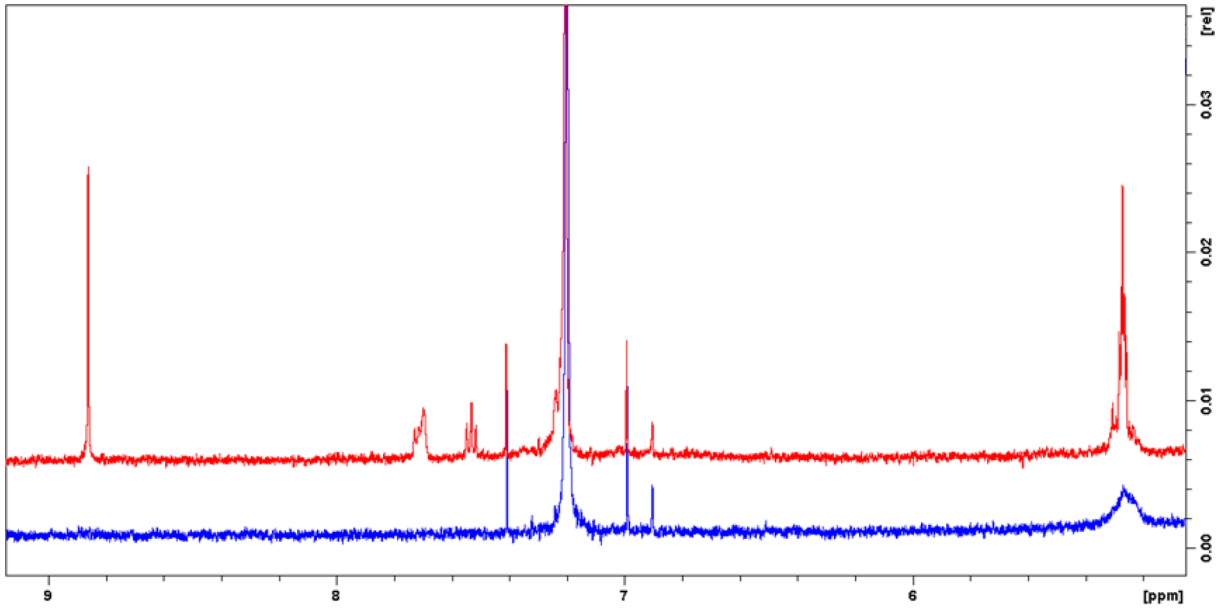

Figure 12. ^{1}H NMR spectra (5−9 ppm region) resulting from the isolated [CdSe{**8**}$_2$] assembly after addition of 2 equiv of **8** under high-dilution conditions to CdSe nanoparticles. Blue: [CdSe{**8**}$_2$] assembly. Red: after addition of dodecanethiol.

from which the porphyrin−nanoparticle conjugates were isolated through flocculation and centrifugation. The solid product could be redissolved in $CDCl_3$. The ^{1}H NMR spectrum was once again totally featureless, essentially identical to Figure 12. Upon addition of dodecanethiol, the broad oleate proton signal at ca. 5 ppm sharpened, indicating their displacement by the monodentate thiol, but, as expected, no porphyrin signal emerged from the baseline. UV/vis spectroscopy confirmed the presence of porphyrin. The data are therefore consistent with the formation of a [CdSe{porphyrin}] assembly in which on average about two porphyrin ligands are irreversibly bound to the nanocrystal surface in tetradentate fashion.

Fluorescence Quenching. All porphyrins in this work induced fluorescence quenching of the quantum dot luminescence. The influence of the porphyrin ligands bearing acid groups was evaluated through comparisons with porphyrin ligands that are not expected to bind (i.e., 5,10,15,20-tetraphenylporphyrinato zinc (**10**) and 5,10,15,20-tetra(4-decyloxyphenyl)porphyrinato zinc (**1**)). The results are shown in Figure 13. For comparison, the effect of a non-porphyrin acid, i.e., 4-nonylbenzoic acid (**11**), is also plotted. All porphyrins show a quenching effect that could not be assigned to FRET. Zenkevich et al.[41] also concluded that non-FRET quenching of fluorescence was operative in their work on 5,10,15,20-tetrapyridylporphyrin−CdSe/ZnS quantum dot nanocomposites. From Figure 13 it is immediately clear that the two nonbinding ligands, **1** and **10**, have a very different profile from the other, binding ligands. Although NMR spectroscopy demonstrated that porphyrin **5** did not form

DOI: 10.1021/acs.inorgchem.5b00892
Inorg. Chem. 2015, 54, 7368−7380

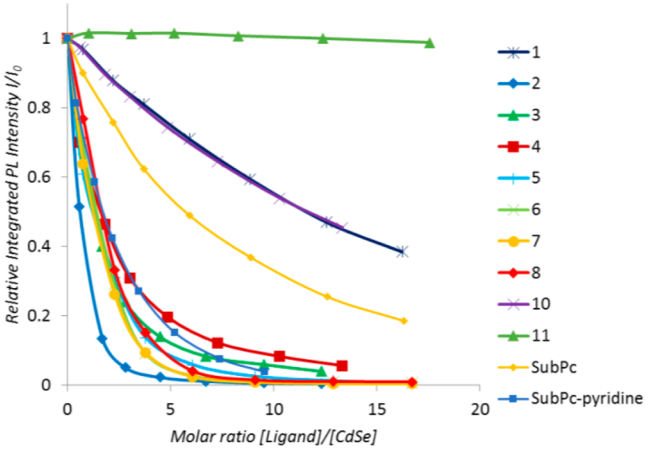

Figure 13. Comparison of the fluorescence quenching effects of porphyrins **1**–**10** in this study, as well as of tris(ethynylpyridine)-subphthalocyanine **I** in comparison with unsubstituted subphthalocyanine. 4-Nonylbenzoic acid (**11**) is included for comparison purposes.

stable, long-lived adducts, the fluorescence quenching effect is on a par with binding porphyrins; at least a fleeting association has to be present to account for the observed quenching. However, these results illustrate that fluorescence alone cannot be used reliably as a measure for ligand exchange processes.

The quenching data are presented as Stern–Volmer plots, Figure 14. All plots, except those of **1** and **10**, deviate substantially from linearity. This is a characteristic feature of the Stern–Volmer plot associated with combined dynamic and static quenching of the fluorophore. The tether chain length appears to influence the extent of quenching, as shown in Figures 14b and 14c. Within the series of monocarboxylate porphyrins, compound **3** with a 6-carbon tether is more effective than **4** (11-carbon chain). Indeed the most effective porphyrin in this work is compound **2**, which lacks an alkyl linker between the ring and the −COOH function. This suggests that the proximity of the porphyrin ring to the nanoparticle plays an important role in the quenching efficiency.

CONCLUSION

The results confirm the picture of CdSe nanocrystals generated by phosphorus-free synthesis methods of a $(CdSe)_x$ core surrounded by a CdX_2 layer, where X = oleate. While tridentate N-donors like pyridyl-substituted subphthalocyanines proved unable to form identifiable nanocrystal/macrocycle conjugates, monodentate zinc porphyrinates bearing one carboxylic acid effectively displace oleate ligands and give high surface coverage. Defined nanoparticle assemblies with only two porphyrins per quantum dot can be obtained under high-dilution conditions, provided the carboxylate donors are linked to the ring by sufficiently long tethers to enable displacement of oleates and binding of the porphyrin parallel to the crystal surface. For ease of quantitative determination of ligand binding by ^{1}H NMR integration, it proved important to release all bound ligands by treatment with excess alkyl thiol, to overcome the problems of line broadening. [CdSe{porphyrin}$_2$] assemblies are also obtainable using porphyrin tetrathiolates; in such cases the S-function needs to be protected and the protection group removed only immediately prior to the reaction with the nanocrystals, under anaerobic conditions. However, once formed, the binding of such tetrathiolato porphyrins is irreversible, even in the presence of excess dodecanethiol.

EXPERIMENTAL PROCEDURES

1-Octadecene tech. 90%, oleic acid 99%, and cadmium oxide (Puratronics 99.998%) were sourced from Alfa-Aesar. Octadecylamine, selenium 100 mesh 99.5+%, and 1-dodecanethiol ≥98% were obtained from Aldrich. Methyl 5-formylsalicylate was obtained from TCI.

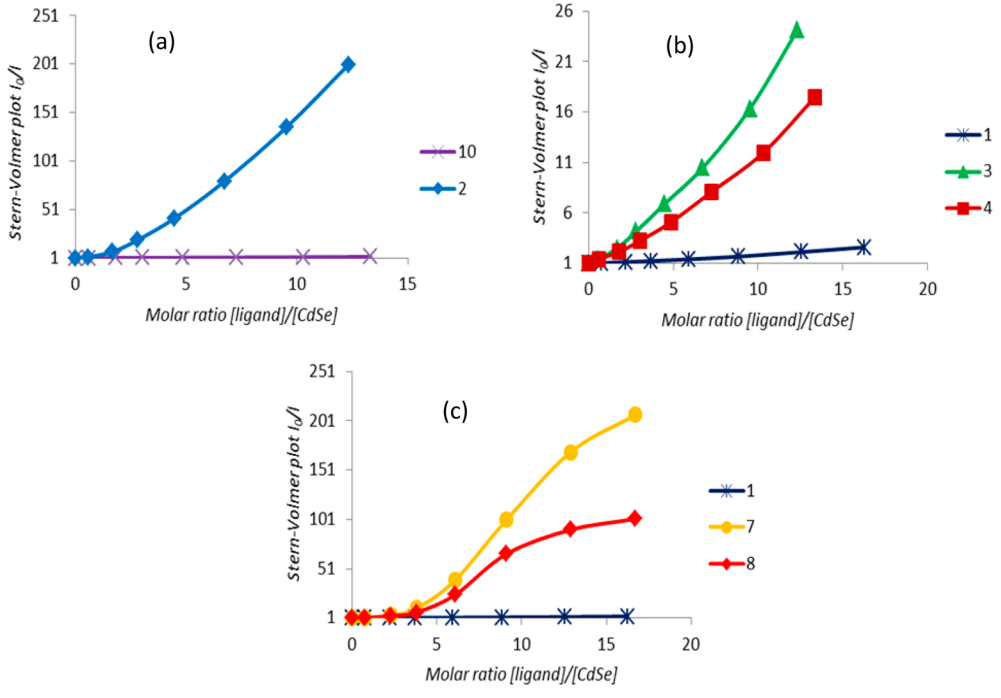

Figure 14. Stern–Volmer plots of CdSe/porphyrin systems for porphyrins **1**–**10**.

DOI: 10.1021/acs.inorgchem.5b00892
Inorg. Chem. 2015, 54, 7368–7380

Unless specified, solvents and chemicals were stored at ambient laboratory conditions and used without further purification. ^{1}H NMR spectra were obtained on Bruker Avance 500 or 300 MHz NMR spectrometers. $CDCl_3$ was used as solvent unless specified. Spectra were referenced to the residual solvent peaks, δ 7.26 for $CDCl_3$. UV/vis absorption spectra of solutions were recorded on a Hitachi U3000 spectrophotometer using the stated solvents. MALDI-TOF mass spectra were measured using a Shimadzu Biotech MALDI mass spectrometer using *trans*-2-[3-(4-*tert*-butylphenyl)-2-methyl-2-propenylidene]malononitrile (DCTB) as matrix. Fluorescence emission spectra were obtained using a PerkinElmer LS55 spectrophotofluorimeter. Elemental microanalyses were carried out at London Metropolitan University. Transmission electron microscopy (TEM) images were obtained on a FEI Tecnai 20 TEM or Jeol JEM 2000-Ex microscope. TEM samples were prepared by dipping a carbon-coated 300 mesh copper grid into a solution of CdSe nanoparticles in dichloromethane. The solvent was evaporated, and TEM micrographs were taken. Compound **1** was prepared from 4-hydroxybenzaldehyde, bromodecane, and pyrrole.[38] The tris(alkynylpyridine)-subphthalocyanine[42] **I** and 5-(4-carboxyphenyl)-10,15,20-triphenyl-porphyrinato zinc[43] (**2**) were prepared following literature procedures. For the syntheses of porphyrin complexes **3**–**9** see the Supporting Information.

Preparation of CdSe Nanocrystals. CdSe nanocrystals were produced by a modification of a literature procedure.[24] To cadmium oxide (300 mg, 2.34 mmol) in octadecene (20 mL) was added oleic acid (2 mL). The mixture was stirred under vacuum for 10 min, and then N_2 was introduced. The mixture was heated to 250 °C and stirred at this temperature until a clear solution was obtained, which was then left to cool to ca. 120 °C. Selenium powder (100 mg, 1.27 mmol) was added and the mixture heated to 240 °C, causing the color to change from yellow to orange. Heating was stopped when the color of the solution was deemed the right shade of orange for the desired nanocrystal size (after various experimental trials). The solution was immediately cooled on an ice bath, and toluene (10 mL) was added. The solution was then transferred to two large centrifuge tubes with filtration (syringe filter: 0.22 μL). The volume of both tubes was adjusted to 30 mL with toluene. The addition of acetone (20 mL) caused the formation of a white precipitate of unreacted starting material. The tubes were centrifuged (1400 rpm), the orange solutions were collected, and the white precipitate was discarded. The solution (25 mL) was again placed in a large centrifuge tube. Methanol (25 mL) was added, followed by centrifugation. An orange oil separated at the bottom, which was collected; the clear top solvent layer was discarded. This process was repeated until all the solution was processed in this way. The separated orange oils were combined and transferred to a smaller centrifuge tube with toluene (total volume 7 mL). Methanol (7 mL) was added and the tube centrifuged. Again the orange oil was decanted. The volume was made up to 7 mL in dichloromethane, and the same volume of ethanol was added, followed by centrifugation. This process was repeated until a thick orange oil or powder was obtained. Finally, acetone (14 mL) was added, and the tube was sonicated for several minutes and then centrifuged. This was repeated five times. A free-flowing orange powder was finally obtained after drying under vacuum and stored under N_2. Yield of CdSe nanocrystals (dried): 113 mg. ^{1}H NMR ($CDCl_3$, 500 MHz): δ 5.19–5.38 (br s, 2H), 1.89–2.06 (br s, 4H), 1.63–1.81 (br s, 4H), 1.14–1.4 (br s, H), 0.81–0.92 (br s, 3H). The size of the obtained nanocrystals was established by UV/vis spectroscopy and confirmed by TEM.

Preparation of Coated [CdSe{(7–9)}] Nanoassemblies. A sample of CdSe QDs (ca. 20 mg) was dissolved in dichloromethane (500 mL) in a volumetric flask. The concentration was established from the UV absorption spectrum. The solution was then transferred to a round-bottom flask, and nitrogen was bubbled through the solution with stirring for 10 min. A solution of porphyrins (**7**, **8**) in dichloromethane (1 mL) was prepared and slowly added over 24 h by the use of a syringe pump (0.7 μL/min). When addition was complete, the content of the flask was transferred to a volumetric flask and the volume adjusted to 500 mL. A UV spectrum was obtained. Most of the solvent was then removed under reduced pressure. The remaining solution was transferred to a centrifuge tube, methanol added to flocculate the nanoparticles, and the tube centrifuged. The solid was separated. Acetone was added and the tube sonicated for 5 min, followed by centrifugation. This was repeated as necessary until the UV spectra of the washing were free of porphyrin. The solid sample could then be redissolved in a suitable NMR solvent.

Porphyrin (**9**) bearing thioacetate chains must be deprotected prior to addition to the nanoparticles. The following procedure was used. All solvents and reagents were degassed and placed under N_2 before use. The porphyrin was dissolved in dichloromethane under N_2. A few drops of an aqueous solution of NaOH (2 M) and methanol were added to the porphyrin with stirring at room temperature. A precipitate formed. When no porphyrin remained in solution, the solvent was removed via a syringe. Acetic acid was added and the mix stirred for 5 min. The acid was removed via a syringe. Methanol was added and the mix stirred for 5 min. The solvent was removed via a syringe. The methanol wash was repeated. Finally CH_2Cl_2 (1 mL) was added. The deprotected porphyrin dissolved, and the solution was transferred to a syringe and was slowly added to CdSe nanoparticles as described above.

■ ASSOCIATED CONTENT

Supporting Information

Experimental and spectroscopic characterization data of the syntheses of porphyrin compounds, luminescence studies, and quantum yields. The Supporting Information is available free of charge on the ACS Publications website at DOI: 10.1021/acs.inorgchem.5b00892.

■ AUTHOR INFORMATION

Corresponding Authors

*E-mail: A.Cammidge@uea.ac.uk.
*E-mail: m.bochmann@uea.ac.uk.

Notes

The authors declare no competing financial interest.

■ ACKNOWLEDGMENTS

This work was supported by the Leverhulme Trust (RPG-197). We thank Dr. C. MacDonald for assistance with transmission electron microscopy. C.B. and S.R.-B. thank the University of East Anglia for studentships.

■ REFERENCES

(1) (a) Zhang, Z.; Horsch, M. A.; Lamm, M. H.; Glotzer, S. C. *Nano Lett.* **2003**, *3*, 1341–1346. (b) Talapin, D. V. *ACS Nano* **2008**, *2*, 1097–1100. (c) Talapin, D. V.; Lee, J.; Kovalenko, M. V.; Shevchenko, E. V. *Chem. Rev.* **2010**, *110*, 389–458. (d) Grzelczak, M.; Vermant, J.; Furst, E. M.; Liz-Marzán, L. M. *ACS Nano* **2010**, *4*, 3591–3605. (e) Arumugam, P.; Xu, H.; Srivastava, S.; Rotello, V. M. *Polym. Int.* **2007**, *56*, 461–466. (f) Kotov, N. A.; Stellacci, F. *Adv. Mater.* **2008**, *20*, 4221–4222. (g) Kotov, N. A. *J. Mater. Chem.* **2011**, *21*, 16673–16674. (h) Liu, K.; Nie, Z.; Zhao, N.; Li, W.; Rubinstein, M.; Kumacheva, E. *Science* **2010**, *329*, 197–200.

(2) (a) Sanchez, C.; Belleville, P.; Popall, M.; Nicole, L. *Chem. Soc. Rev.* **2011**, *40*, 696–753. (b) Wang, L. B.; Xu, L. G.; Kuang, H.; Xu, C. L.; Kotov, N. A. *Acc. Chem. Res.* **2012**, *45*, 1916–1926. (c) Xu, L. G.; Ma, W.; Wang, L.; Xu, C. L.; Kuang, H.; Kotov, N. A. *Chem. Soc. Rev.* **2013**, *42*, 3114–3126.

(3) (a) Pileni, M. P. *Acc. Chem. Res.* **2008**, *41*, 1799–1809. (b) Wang, T.; Zhuang, J.; Lynch, J.; Chen, O.; Wang, Z. L.; Wang, X. R.; La Montagne, D.; Wu, H. M.; Wang, Z. W.; Cao, Y. C. *Science* **2012**, *338*, 358–363. (c) Boles, M. A.; Talapin, D. V. *J. Am. Chem. Soc.* **2014**, *136*, 5868–5871.

(4) (a) Peng, X.; Wilson, T. E.; Alivisatos, A. P.; Schultz, P. G. *Angew. Chem., Int. Ed. Engl.* **1997**, *36*, 145–147. (b) DeVries, G. A.; Brunnbauer, M.; Hu, Y.; Jackson, A. M.; Long, B.; Neltner, B. T.;

DOI: 10.1021/acs.inorgchem.5b00892
Inorg. Chem. 2015, 54, 7368–7380

Uzun, O.; Wunsch, B. H.; Stellacci, F. *Science* **2007**, *315*, 358−361. (c) Reguera, J.; Kim, H.; Stellacci, F. *Chimia* **2013**, *67*, 811−818 and cited references .
(5) (a) Worden, J. G.; Shaffer, A. W.; Huo, Q. *Chem. Commun.* **2004**, 518−519. (b) Wilson, R.; Chen, Y.; Aveyard, J. *Chem. Commun.* **2004**, 1156−1157. (c) Sung, K.-M.; Mosley, D. W.; Peelle, B. R.; Zhang, S.; Jacobson, J. M. *J. Am. Chem. Soc.* **2004**, *126*, 5064−5065. (d) Dai, Q.; Worden, J. G.; Trullinger, J.; Huo, Q. *J. Am. Chem. Soc.* **2005**, *127*, 8008−8009. (e) Levy, R.; Wang, Z.; Duchesne, L.; Doty, R. C.; Cooper, A. I.; Brust, M.; Fernig, D. *ChemBioChem* **2006**, *7*, 592−594. (f) Sharma, J.; Chhabra, R.; Andersen, C. S.; Gothelf, K. V.; Yan, H.; Liu, Y. *J. Am. Chem. Soc.* **2008**, *130*, 7820−7821. (g) Wang, Q. B.; Wang, H.; Lin, C. X.; Sharma, J.; Zou, S.; Liu, Y. *Chem. Commun.* **2010**, *46*, 240−242.
(6) Review: Green, M. *J. Mater. Chem.* **2010**, *20*, 5797−5809.
(7) Taylor, J.; Kippeny, T.; Rosenthal, S. J. *J. Cluster Sci.* **2001**, *12*, 571−582.
(8) Kopping, J. T.; Patten, T. E. *J. Am. Chem. Soc.* **2008**, *130*, 5689−5698.
(9) (a) Kalyuzhny, G.; Murray, R. W. *J. Phys. Chem. B* **2005**, *109*, 7012−7021. (b) Evans, C. M.; Evans, M. E.; Krauss, T. D. *J. Am. Chem. Soc.* **2010**, *132*, 10973−10975. (c) Newton, J. C.; Ramasamy, K. R.; Mandal, M.; Joshi, G. K.; Kumbhar, A.; Sardar, R. *J. Phys. Chem. C* **2012**, *116*, 4380−4389.
(10) (a) Morris-Cohen, A. J.; Donakowski, M. D.; Knowles, K. E.; Weiss, E. A. *J. Phys. Chem. C* **2010**, *114*, 897−906. (b) Morris-Cohen, A. J.; Frederick, M. T.; Lilly, G. D.; McArthur, E. A.; Weiss, E. A. *J. Phys. Chem. Lett.* **2010**, *1*, 1078−1081. (c) Wang, F.; Buhro, W. E. *J. Am. Chem. Soc.* **2012**, *134*, 5369−5380.
(11) Garcia-Rodriguez, R.; Hendricks, M. P.; Cossairt, B. M.; Liu, H.; Owen, J. S. *Chem. Mater.* **2013**, *25*, 1233−1249.
(12) Gomes, R.; Hassinen, A.; Szczygiel, A.; Zhao, Q. A.; Vantomme, A.; Martins, J. C.; Hens, Z. *J. Phys. Chem. Lett.* **2011**, *2*, 145−152.
(13) Owen, J. S.; Park, J.; Trudeau, P. E.; Alivisatos, A. P. *J. Am. Chem. Soc.* **2008**, *130*, 12279−12281.
(14) Reviews: (a) Morris-Cohen, A. J.; Malicki, M.; Peterson, M. D.; Slavin, J. W. J.; Weiss, E. A. *Chem. Mater.* **2013**, *25*, 1155−1165. (b) Hens, Z.; Martins, J. C. *Chem. Mater.* **2013**, *25*, 1211−1221.
(15) (a) Moreels, I.; Fritzinger, B.; Martins, J. C.; Hens, Z. *J. Am. Chem. Soc.* **2008**, *130*, 15081−15086. (b) Fritzinger, B.; Moreels, I.; Lommens, P.; Koole, R.; Hens, Z.; Martins, J. C. *J. Am. Chem. Soc.* **2009**, *131*, 3024−3032. (c) Fritzinger, B.; Capek, R. K.; Lambert, K.; Martins, J. C.; Hens, Z. *J. Am. Chem. Soc.* **2010**, *132*, 10195−10201. (d) Moreels, I.; Justo, Y.; de Geyter, B.; Haustraete, K.; Martins, J. C.; Hens, Z. *ACS Nano* **2011**, *5*, 2004−2012. (e) Hassinen, A.; Moreels, I.; de Nolf, K.; Smet, P. F.; Martins, J. C.; Hens, Z. *J. Am. Chem. Soc.* **2012**, *134*, 20705−20712. (f) Hassinen, A.; Moreels, I.; de Mello Donega, C.; Martins, J. C.; Hens, Z. *J. Phys. Chem. Lett.* **2010**, *1*, 2577−2581.
(16) (a) Morris-Cohen, A. J.; Vasilenko, V.; Amin, V. A.; Reuter, M. G.; Weiss, E. A. *ACS Nano* **2012**, *6*, 557−565. (b) Lokteva, I.; Radychev, N.; Witt, F.; Borchert, H.; Parisi, J.; Kolny-Olesiak, J. *J. Phys. Chem. C* **2010**, *114*, 12784−12791. (c) Anderson, N. C.; Hendricks, M. P.; Choi, J. J.; Owen, J. S. *J. Am. Chem. Soc.* **2013**, *135*, 18536−18548.
(17) (a) Munro, A. M.; Jen-La Plante, I.; Ng, M. S.; Ginger, D. S. *J. Phys. Chem. C* **2007**, *111*, 6220−6227. (b) Li, X.; Nichols, V. M.; Zhou, D.; Lim, C.; Pau, G. S. H.; Bardeen, C. J.; Tang, M. L. *Nano Lett.* **2014**, *14*, 3382−3387. (c) Mehta, A.; Sharma, S. N.; Chawla, P.; Chand, S. *Colloid Polym. Sci.* **2014**, *292*, 301−315.
(18) Knittel, F.; Gravel, E.; Cassette, E.; Pons, T.; Pillon, F.; Dubertret, B.; Doris, E. *Nano Lett.* **2013**, *13*, 5075−5078.
(19) (a) Zhang, W. J.; Chen, G. J.; Wang, J.; Ye, B. C.; Zhong, X. H. *Inorg. Chem.* **2009**, *48*, 9723−9731. (b) Liu, L.; Guo, X. H.; Li, Y.; Zhong, X. H. *Inorg. Chem.* **2010**, *49*, 3768−3775. (c) Kalita, M.; Cingarapu, S.; Roy, S.; Park, S. C.; Higgins, D.; Jankowiak, R.; Chikan, V.; Klabunde, K. J.; Bossmann, S. H. *Inorg. Chem.* **2012**, *51*, 4521−4526.
(20) (a) Susumu, K.; Uyeda, H. T.; Medintz, I. L.; Pons, T.; Delehanty, J. B.; Mattoussi, H. *J. Am. Chem. Soc.* **2007**, *129*, 13987. (b) Ip, A. H.; Thon, S. M.; Hoogland, S.; Voznyy, O.; Zhitomirsky, D.; Debnath, R.; Levina, L.; Rollny, L. R.; Carey, G. H.; Fischer, A.; Kemp, K. W.; Kramer, I. J.; Ning, Z.; Labelle, A. J.; Chou, K. W.; Amassian, A.; Sargent, E. H. *Nat. Nanotechnol.* **2012**, *7*, 577−582. (c) Hughes, B. K.; Ruddy, D. A.; Blackburn, J. L.; Smith, D. K.; Bergren, M. R.; Nozik, A. J.; Johnson, J. C.; Beard, M. C. *ACS Nano* **2012**, *6*, 5498−5506. (d) Bian, T.; Shang, L.; Yu, H.; Perez, M. T.; Wu, L. Z.; Tung, C. H.; Nie, Z.; Tang, Z.; Zhang, T. *Adv. Mater.* **2014**, *26*, 5613−5618. (e) Mobarok, M. H.; Buriak, J. M. *Chem. Mater.* **2014**, *26*, 4653−4661.
(21) Tavasoli, E.; Guo, Y.; Kunal, P.; Grajeda, J.; Gerber, A.; Vela, J. *Chem. Mater.* **2012**, *24*, 4231−4241.
(22) (a) Remiro-Buenamañana, S.; Diaz-Moscoso, A.; Hughes, D. L.; Bochmann, M.; Tizzard, G. J.; Coles, S. J.; Cammidge, A. N. *Angew. Chem., Int. Ed.* **2015**, *54*, 7510−7514. (b) Alharbi, N.; Diaz-Moscoso, A.; Tizzard, G. J.; Coles, S. J.; Cook, M. J.; Cammidge, A. N. *Tetrahedron* **2014**, *70*, 7370−7379. (c) Garland, A. D.; Bryant, G. C.; Chambrier, I.; Cammidge, A. N.; Cook, M. J. *J. Porphyrins Phthalocyanines* **2014**, *18*, 944−949. (d) Pal, C.; Sharma, A. K.; Cammidge, A. N.; Cook, M. J.; Ray, A. K. *J. Phys. Chem. B* **2013**, *117*, 15033−15040. (e) Heeney, M. J.; Al-Raqa, S. A.; Auger, A.; Burnham, P. M.; Cammidge, A. N.; Chambrier, I.; Cook, M. J. *J. Porphyrins Phthalocyanines* **2013**, *17*, 649−664. (f) Mack, J.; Sosa-Vargas, L.; Coles, S. J.; Tizzard, G. J.; Chambrier, I.; Cammidge, A. N.; Cook, M. J.; Kobayashi, N. *Inorg. Chem.* **2012**, *51*, 12820−12833. (g) Zhang, L.; Hughes, D. L.; Cammidge, A. N. *J. Org. Chem.* **2012**, *77*, 4288−4297. (h) Pal, C.; Cammidge, A. N.; Cook, M. J.; Sosa-Sanchez, J. L.; Sharma, A. K.; Ray, A. K. *J. R. Soc., Interface* **2012**, *9*, 183−189. (i) Chaure, N. B.; Pal, C.; Barard, S.; Kreouzis, T.; Ray, A. K.; Cammidge, A. N.; Chambrier, I.; Cook, M. J.; Murphy, C. E.; Cain, M. G. *J. Mater. Chem.* **2012**, *22*, 19179−19189. (j) Cammidge, A. N.; Nekelson, F.; Hughes, D. L.; Zhao, Z. X.; Cook, M. J. *J. Porphyrins Phthalocyanines* **2010**, *14*, 1001−1011. (k) Zhao, Z. X.; Cammidge, A. N.; Hughes, D. L.; Cook, M. J. *Org. Lett.* **2010**, *12*, 5138−5141. (l) Zhao, Z. X.; Cammidge, A. N.; Cook, M. J. *Chem. Commun.* **2009**, 7530−7532. (m) Khene, S.; Cammidge, A. N.; Cook, M. J.; Nyokong, T. *J. Porphyrins Phthalocyanines* **2007**, *11*, 761−770. (n) Cammidge, A. N.; Scaife, P. J.; Berber, G.; Hughes, D. L. *Org. Lett.* **2005**, *7*, 3413−3416.
(23) Claessens, C. G.; González-Rodríguez, D.; Torres, T. *Chem. Rev.* **2002**, *102*, 835−854.
(24) Jasieniak, J.; Bullen, C.; van Embden, J.; Mulvaney, P. *J. Phys. Chem. B* **2005**, *109*, 20665−20668.
(25) (a) Peng, Z. A.; Peng, X. *J. Am. Chem. Soc.* **2001**, *123*, 183−184. (b) Nordell, K. J.; Boatman, E. M.; Lisensky, G. C. *J. Chem. Educ.* **2005**, *82*, 1697−1699. (c) Yang, Y. A.; Wu, H.; Williams, K. R.; Cao, Y. C. *Angew. Chem.* **2005**, *117*, 6870−6873.
(26) CdSe nanocrystals of 2−2.5 nm diameter suffer from low TEM contrast, and as has been observed before, size determination by TEM measurements is challenging, see ref 9c.
(27) Yu, W. W.; Qu, L. H.; Guo, W. H.; Peng, X. G. *Chem. Mater.* **2003**, *15*, 2854−2860.
(28) Williams, A. T. R.; Winfield, S. A.; Miller, J. N. *Analyst* **1983**, *108*, 1067−1071.
(29) Based on photoluminescence quenching, the lower limit of the alkanethiol binding constant to CdSe has been estimated as 10^9 L/mol, ref 17c.
(30) Ji, X. H.; Copenhaver, D.; Sichmeller, C.; Peng, X. *J. Am. Chem. Soc.* **2008**, *130*, 5726−5735.
(31) Takeuchi, H.; Omogo, B.; Heyes, C. D. *Nano Lett.* **2013**, *13*, 4746−4752.
(32) Anderson, N. C.; Owen, J. C. *Chem. Mater.* **2013**, *25*, 69−76.
(33) (a) Qu, L. H.; Peng, X. *J. Am. Chem. Soc.* **2002**, *124*, 2049−2055. (b) Jasieniak, J.; Mulvaney, P. *J. Am. Chem. Soc.* **2007**, *129*, 2841−2848.
(34) Tomoaia-Cotisel, M.; Zsako, J.; Mocanu, A.; Lupea, M.; Chifu, E. *J. Colloid Interface Sci.* **1987**, *117*, 464−476.

DOI: 10.1021/acs.inorgchem.5b00892
Inorg. Chem. 2015, 54, 7368−7380

(35) Zenkevich, E. I.; von Borczyskowski, C. *J. Porphyrins Phthalocyanines* **2014**, *18*, 1−19.
(36) (a) Zenkevich, E. I.; Cichos, F.; Shulga, A.; Petrov, E. P.; Blaudeck, T.; von Borczyskowski, C. *J. Phys. Chem. B* **2005**, *109*, 8679−8692. (b) Zenkevich, E. I.; Blaudeck, T.; Shulga, A.; Cichos, F.; von Borczyskowski, C. *J. Lumin.* **2007**, *122*−*123*, 784−788. (c) Blaudeck, T.; Zenkevich, E. I.; Cichos, F.; von Borczyskowski, C. *J. Phys. Chem. C* **2008**, *112*, 20251−20257. (d) Blaudeck, T.; Zenkevich, E. I.; Abdel-Mottaleb, M.; Szwaykowska, K.; Kowerko, D.; Cichos, F.; von Borczyskowski, C. *ChemPhysChem* **2012**, *13*, 959−972. (e) Zenkevich, E. I.; Stupak, A. P.; Kowerko, D.; von Borczyskowski, C. *Chem. Phys.* **2012**, *406*, 21−29.
(37) (a) Frasco, M. F.; Vamvakaki, V.; Chaniotakis, N. *J. Nanopart. Res.* **2010**, *12*, 1449−1458. (b) Keane, P. M.; Gallagher, S. A.; Magno, L. M.; Leising, M. J.; Clark, I. P.; Greetham, G. M.; Towrie, M.; Gun'ko, Y. K.; Kelly, J. M.; Quinn, S. J. *Dalton Trans.* **2012**, *41*, 13159−13166. (c) Lemon, C. M.; Karnas, E.; Bawendi, M. G.; Nocera, D. G. *Inorg. Chem.* **2013**, *52*, 10394−10406.
(38) Kugimiya, S.; Takemura, M. *Tetrahedron Lett.* **1990**, *31*, 3157−3160.
(39) The redox metalation of porphyrins by binding to metal surfaces has been observed: Goldoni, A.; Pignedoli, C. A.; Di Santo, G.; Castellarin-Cudia, C.; Magnano, E.; Bondino, F.; Verdini, A.; Passerone, D. *ACS Nano* **2012**, *6*, 10800−10807.
(40) Kanehara, M.; Teranishi, T. *e-J. Surf. Sci. Nanotechnol.* **2005**, *3*, 30−32.
(41) Zenkevich, E. I.; Blaudeck, T.; Milekhin, A.; von Borczyskowski, C. *Int. J. Spectrosc.* **2012**, 971791 DOI: 10.1155/2012/971791.
(42) Łapok, Ł.; Claessens, C. G.; Wohrle, D.; Torres, T. *Tetrahedron Lett.* **2009**, *50*, 2041−2044.
(43) Fanti, C.; Monti, D.; La Monica, L.; Ceccacci, F.; Mancini, G.; Paolesse, G. *J. Porphyrins Phthalocyanines* **2003**, *7*, 112−119.

DOI: 10.1021/acs.inorgchem.5b00892
Inorg. Chem. 2015, 54, 7368−7380